Articles

A New Class of Symmetric Bisbenzimidazole-Based DNA Minor Groove-Binding Agents Showing Antitumor Activity

John Mann,[†,‡] Anne Baron,[†,‡] Yaw Opoku-Boahen,[†] Eric Johansson,[||] Gary Parkinson,[||] Lloyd R. Kelland,[§] and Stephen Neidle*[,||]

Chemistry Department, Reading University, Whiteknights, Reading RG6 6AD, U.K., CRC Centre for Cancer Therapeutics, Institute of Cancer Research, Sutton, Surrey SM2 5NG, U.K., and CRC Biomolecular Structure Unit, Chester Beatty Laboratories, Institute of Cancer Research, 237 Fulham Road, London SW3 6JB, U.K.

Received July 17, 2000

The synthesis and evaluation of the novel head-to-head bisbenzimidazole compound 2,2-bis-[4′-(3″-dimethylamino-1″-propyloxy)phenyl]-5,5-bi-1*H*-benzimidazole is described. An X-ray crystallographic study of a complex with the DNA dodecanucleotide sequence d(CGCGAATTCGCG) shows the compound bound in the A/T minor groove region of a B-DNA duplex and that the head-to-head bisbenzimidazole motif hydrogen-bonds to the edges of all four consecutive A:T base pairs. The compound showed potent growth inhibition with a mean IC_{50} across an ovarian carcinoma cell line panel of 0.31 μM, with no significant cross-resistance in two acquired cisplatin-resistant cell lines and a low level of cross-resistance in the P-glycoprotein overexpressing acquired doxorubicin-resistant cell line. Studies with the hollow fiber assay and in vivo tumor xenografts showed some evidence of antitumor activity.

Introduction

Studies on the noncovalent interactions of small molecules with the minor groove of DNA continue to be a fruitful area for the discovery of potential new therapeutic agents. Those compounds based on bis(phenylamidinium)furans can have activity[1−4] against *Pneumocystis carinii*, a pathogen of major clinical importance in the treatment of AIDS patients, as well as cytotoxic activity against tumor cell lines.[5] Others have demonstrated experimental antitumor activity, notably the synthetic compound[6] PNU-166196 (an α-bromoacrylic derivative of distamycin) and various asymmetric bisbenzimidazole compounds.[7] The parent of this latter family is the cell stain Hoechst 33258, also known as Pibenzimol (Figure 1), which has two benzimidazole groups linked in a head-to-tail manner.[7] This compound was initially found to have activity against L1210 murine leukemia,[8] which was followed by several phase I trials in humans.[9] The first trial was limited by pancreatic toxicity, although in a second trial some responses were seen in pancreatic cancer; a subsequent phase II trial did not show any objective responses,[10] and no further trials of this agent have been reported. Hoechst 33258 is weakly mutagenic in *Salmonella* test strains.[11,12] It inhibits the binding of TATA-box binding protein to DNA[13] and is an effective inhibitor of mammalian DNA topoisomerase I.[14]

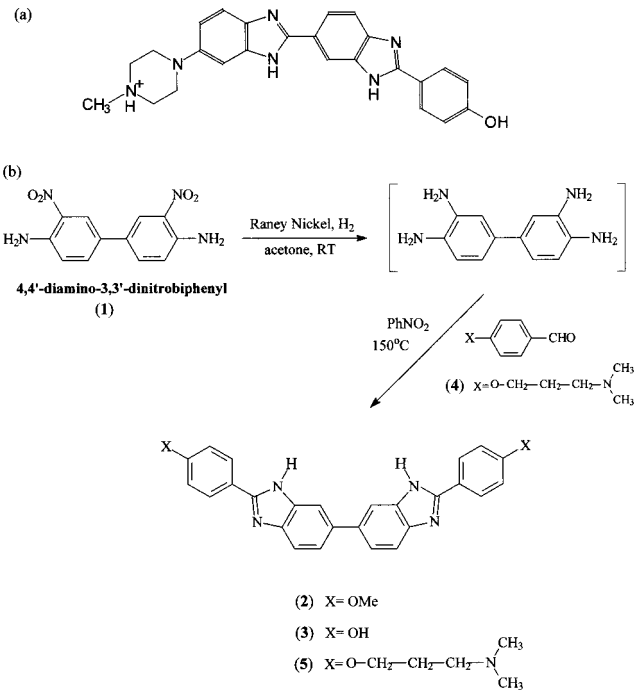

Figure 1. (a) Structure of Hoechst 33258. (b) Synthetic scheme used in the synthesis of the lead compound **5**.

Hoechst 33258 recognizes A/T sequences.[15] The mode of binding to DNA has been established from X-ray crystallographic studies of complexes with several A/T-containing oligonucleotides,[16,17] as well as NMR studies in solution.[18,19] All of these studies concur in finding that the two core benzimidazole groups of Hoechst 33258 together recognize three consecutive A:T base pairs, via a pair of bifurcated hydrogen bonds, with van der Waals

* To whom correspondence should be addressed. Tel: 0044 020 7970 6043. Fax: 0044 020 7 352 8039. E-mail at s.neidle@icr.ac.uk.
† Reading University.
§ CRC Centre for Cancer Therapeutics.
|| CRC Biomolecular Structure Unit.
‡ Present address: School of Chemistry, Queen's University Belfast, Belfast BT9 5AG, U.K.

10.1021/jm000297b CCC: $20.00
Published on Web 12/07/2000

forces playing a major role in the overall binding.[20] A number of other head-to-tail linked benzimidazoles have been studied as probes of minor groove recognition, and all show the same pattern of base recognition,[21−23] including compounds with three benzimidazole units.[24−27] We hypothesized that the size of the binding site could be extended by a symmetric head-to-head arrangement for the two benzimidazole groups. Several such molecules were subsequently synthesized and shown by DNA footprinting and X-ray crystallographic methods to bind to A/T DNA sequences in this manner.[28] It was also suggested that replacement of the piperazine group in Hoechst 33258 by pure DNA-binding groups would enhance cytotoxicity and possibly lead to compounds with antitumor activity yet lacking the toxicity of Hoechst 33258. We report here a detailed biological evaluation of the lead compound 2,2-bis[4′-(3″-dimethylamino-1″-propyloxy)phenyl]-5,5-bi-1*H*-benzimidazole (**5**; Figure 1b) in the series, together with synthetic and structural studies.

Results

Chemistry. The required bisbenzimidazoles were synthesized via the route shown in Figure 1b. This involved condensation between 3,3′,4,4′-tetraaminobiphenyl (prepared by Raney nickel reduction of 3,3′-dinitro-4,4′-diaminobiphenyl (**1**)[28]) and the requisite aromatic aldehyde by refluxing the reactants in nitrobenzene under argon at 150 °C for 8−12 h. Thus 4-methoxybenzaldehyde yielded bisbenzimidazole (**2**) (29%); 4-hydroxybenzaldehyde provided compound **3** (23%); and 4-(3′-dimethylamino-1′-propyloxy)benzaldehyde (**4**) yielded compound **5** (35%). This last aldehyde was itself synthesized via a Mitsunobu reaction between 4-hydroxybenzaldehyde and 3-dimethylaminopropan-1-ol (Ph_3P, DEAD, THF, 85%).

Crystal Structure Description. The crystallographic analysis confirms that the structure of the complex of compound **5** with the sequence d(CGCGAATTCGCG) is isomorphous with other dodecamers of the same sequence, with or without minor groove-bound drug. The mean helical twist between successive base pairs is 35.6°, and there are 10.1 base pairs/helical turn. The mean rise per base pair is 3.34 Å. Figure 2a shows a temperature factor representation of the complex. The core central bisbenzimidazole region of the drug is well-defined and relatively immobile. However, the temperature factors for the drug side chains are high. This is as expected for long aliphatic chains of this nature, and indeed, the conformation shown is probably only one of several possible ones which could have been fitted to the rather diffuse electron density.

A close-up view of the central benzimidazole region (Figure 2b) illustrates some of the factors that contribute to the binding of the drug. First, the molecule is overall crescent-shaped, thus complementing the helicity of the minor groove. The drug molecule further adapts to the groove curvature by the twisting of its two subunits, with a dihedral angle of 20° between them. Second, the positions of the hydrogen-bond donors on the drug complement that of the acceptor spacing of the DNA. The two benzimidazole groups each hydrogen-bond to two A:T base pairs, in accordance with the initial modeling suggestion, and thus cover all four A:T base pairs in this sequence (Figure 2a). The overall binding site size is 6 base pairs.

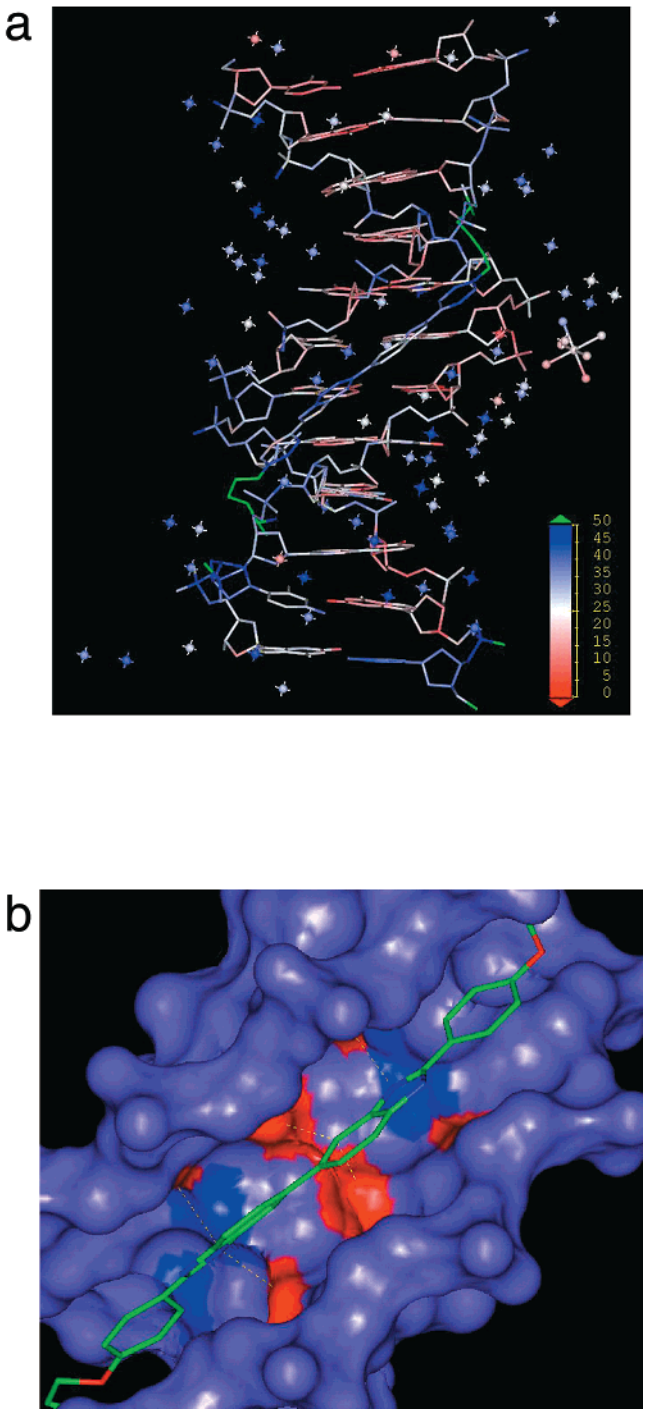

Figure 2. (a) View (drawn with the GRASP program[40]) of the structure of the complex between d(CGCGAATTCGCG) and compound **5**, colored according to temperature factor. Note the high temperature factors of the alkylamino termini of compound **5**, indicating significant mobility. (b) Surface representation of the minor groove region of the complex, showing the binding of compound **5**. Hydrogen bonds to base edges are indicated by dashed lines.

The minor groove widths were calculated with the CURVES program[29] and are shown in Figure 3, compared to those of complexes with other related ligands as well as to that of the native dodecamer. This shows that the overall shape of the minor groove in these structures is similar but that the actual widths vary.

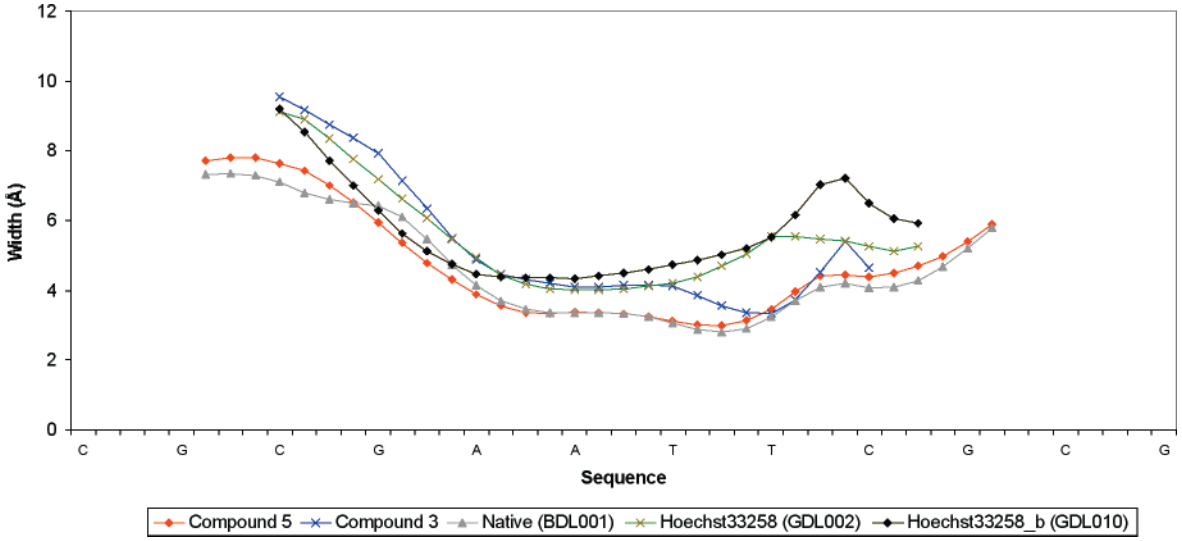

Figure 3. Plot of C4′−C4′ minor groove widths[29] in the complex of d(CGCGAATTCGCG) with compound **5**, compared with those in several other complexes. The Nucleic Acid Database[41] codes are given for the structures.

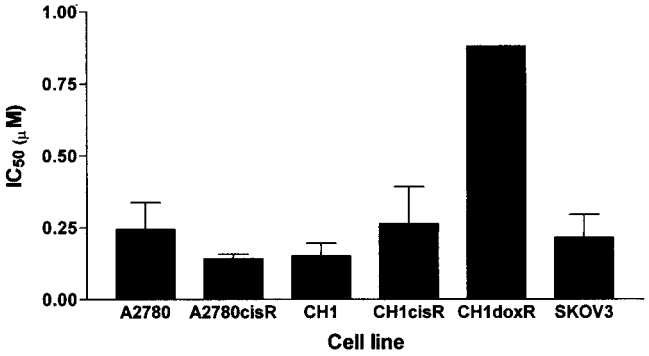

Figure 4. Growth inhibition by compound **5** across a panel of human ovarian carcinoma cell lines using 96-h continuous drug exposure. Values are mean ± SD from 3 experiments.

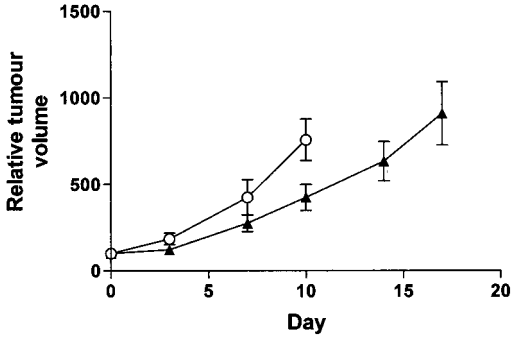

Figure 5. In vivo antitumor activity of compound **5** (4 mg/kg, ip days 0, 4, 8) against CH1 human ovarian carcinoma xenografts: ○, control; ▲, treated group. Data points are mean ± SD.

As can be seen, the minor groove width of the present complex is very similar to that of the native dodecamer, particularly in the narrow AATT region, where the widths are around 3.3 Å. There is a tendency for a greater groove width in other drug−dodecamer structures in the 5′-AATT region, which may be due to the differences in base−drug hydrogen bonding.

Evaluation Against a Human Ovarian Carcinoma Cell Line Panel. The growth inhibitory properties of compound **5** were initially determined using a small panel of human ovarian carcinoma cell lines, including sublines possessing acquired resistance to cisplatin (cisR lines) and doxorubicin (doxR line). Results using 4-day continuous drug exposure are shown in Figure 4. Compound **5** showed potent growth inhibition with a mean IC_{50} across the panel of 0.31 μM. Moreover, there was no marked cross-resistance in two acquired cisplatin-resistant cell lines and only low level cross-resistance in the P-glycoprotein overexpressing acquired doxorubicin-resistant cell line (RF of 5.8 compared to 90 for doxorubicin itself).

Compound **5** has also been evaluated by the National Cancer Institute (NCI) using 60 cell lines which are derived from a diverse group of human cancers.[30] In contrast to the methods outlined above, the NCI used a 48-h drug exposure, albeit followed by the same SRB endpoint. In common with the above results, compound **5** showed potent growth inhibition with a mean GI_{50} across the 60 cell lines of 0.21 μM. Pearson coefficient COMPARE analysis indicated that compound **5** does not share a response pattern with any other agent in the databank (the highest GI_{50} coefficients were 0.661 for MDR Rhod30 and 0.578 for echinomycin). We are grateful to the NCI for communicating these data.

The effect of the time of drug exposure was investigated using the SKOV-3 cell line. There was little dependence on the time of drug exposure to growth inhibition (IC_{50}); values (in μM) were 2 h, 0.33; 6 h, 0.105; 24 h, 0.115; and 96 h, 0.1.

In Vivo Antitumor Activity. Initial in vivo antitumor evaluation of compound **5** used the hollow fiber assay with ip-implanted fibers containing CH1 cells and ip-administered drug.[31] Evidence of antitumor activity was seen following a single dose of 4 mg/kg (T/C of 0.79). Additional hollow fiber studies were also performed by the NCI; a maximum effect of T/C of 0.56 was observed against the OVCAR-3 human ovarian carcinoma cell line (in ip-implanted fibers) using a dose of 4.5 mg/kg given ip daily for 4 consecutive days (Table 1b; personal communication, NCI).

Following the observation of some antitumor effect in mice bearing CH1-containing hollow fibers, compound **5** was evaluated against the corresponding sc xenograft

Table 1.

a. Cytotoxicity of Bisbenzimidazole Compounds for 96-h Exposure in a Panel of Ovarian Cell Lines

		IC_{50} (μM)			
compd	NSC no.	A2780	A2780cisR	CH1	SKOV-3
2	D701062	13.5	5.1	3.8	16.5
3	D699126	4.3	2.7	1.05	16.0
5	D699127	0.235	0.115	0.24	0.375
Hoechst 33258	322921	12.0	9.5	26.5	>100

b. Activity in sc Human Tumor Xenograft (hollow fiber) Assays, as Determined by the NCI[31]

compd	NSC no.	ip score	sc score	total score
2	D701062	8	0	8
3	D699126	10	0	10
5	D699127	12	4	16

using a maximum tolerated dose of 4 mg/kg (days 0, 4, 8 ip administration). Tumor growth curves for treated versus control groups are shown in Figure 5. Compound **5** exhibited some evidence of in vivo antitumor activity against this established sc-implanted xenograft; the maximum T/C% was 0.56 on day 10 (this difference just attained statistical significance *P* of 0.047, two-tailed Students *t*-test). There was no evidence of drug-induced toxicity in this study.

Discussion

Compound **5** possesses promising in vitro antitumor growth inhibitory properties, with the concentration required for 50% inhibition being around 200−300 nM. Table 1a compares activity for **5** with those previously reported by us[28] for compounds **2** and **3**, which shows that compound **5** is consistently 10−20-fold more active in the cell line panel. Furthermore, activity was observed for **5** against two cell lines possessing resistance to the DNA-damaging agent cisplatin and against a P-glycoprotein overexpressing doxorubicin-resistant line. Moreover, the two acquired cisplatin-resistant cell lines are known to be resistant through distinct biochemical mechanisms: A2780cisR, through multiple mechanisms of reduced platinum transport, increased glutathione and increased DNA repair, while CH1cisR increased DNA repair or increased tolerance to platinum−DNA adducts.[32] Time of exposure experiments showed that compound **5** was similarly potent whether drug exposure was short (2 or 6 h) followed by wash-out or long (24 or 96 h). This suggests that in vivo plasma concentrations required for in vitro growth inhibition (around 200 nM) only need to be attained for relatively short periods (2−6 h) for antitumor efficacy to be obtained. This effect is unlikely to be due to pharmacokinetic factors, which would not usually be seen in an in vitro setting but are more probably due to rapid saturation of the drug and retained affinity for DNA. Furthermore, data from the NCI COMPARE analysis suggest that compound **5** does not share a pattern of growth inhibition with any other reported anticancer agents. Antitumor activity was also observed in vivo using the hollow fiber assay and, moreover, against an established sc ovarian cancer xenograft. Using a day 0, 4, 8 schedule, activity was observed at day 10 post start of treatment. The hollow fiber in vivo assay on all three compounds (Table 1b) shows that compound **5** shows a significant (though not outstanding) level of activity, whereas the other two show only very modest responses.

The crystallographic study demonstrates that compound **5** can bind effectively to the A/T-rich minor groove of B-form DNA, in accord with our earlier observations on the dihydroxy derivative **3**.[28] Both compounds are effective inhibitors of transcription,[28] with **5** being an order of magnitude more potent. This parallels the higher affinity for DNA shown by **5** compared to **3**.[28] Although we do not as yet have direct evidence that the in vitro (and possibly the in vivo) properties of **5** are due to its effect on transcription, we suggest that this is a plausible mechanism. However we cannot rule out at this stage alternative DNA-related modes of action such as inhibition of DNA topoisomerases or helicases. Many (though not all) minor groove-binding molecules possessing significant cytotoxicity and antitumor properties also covalent bond in the minor groove (especially to N3 of adenine or N2 of guanine). Compounds such as the alkylating distamycin derivative tallimustine[33] have antitumor activity whereas the parent distamycin does not. However the discovery of in vivo activity for the noncovalent α-bromoacryloyl derivative of distamycin (PNU 151807)[6] has demonstrated that covalent binding to DNA is not always a requirement in order for groove-binding molecules to have antitumor activity, a conclusion reinforced by the present results on compound **5**. In the head-to-head bisbenzimidazole category, a number of nonalkylating cytotoxic analogues have been reported, some of which may target human tumor helicases.[34]

Experiments are underway to further investigate these findings on compound **5**, as well as to design more active analogues.

Experimental Section

2,2-Bis(4′-methoxyphenyl)-5,5-bi-1*H*-benzimidazole (2). 4,4′-Diamino-3,3′-dinitrobiphenyl (2 g, 7.3 mmol) (**1**) in acetone (70 mL) was reduced by hydrogenation using 40 psi of H_2 and a catalytic amount of Raney nickel for 2 h. After filtration the solvent was removed under reduced pressure to obtain a brown solid which was used in the next step without further purification. The crude intermediate and *p*-anisaldehyde (1.8 mL, 14.6 mmol) in nitrobenzene (20 mL) were heated at 150 °C under argon for 8 h. An excess of hexane (40 mL) was added to the cooled mixture to afford a precipitate and this was removed by filtration. The precipitate was then purified by column chromatography on silica gel (gradient from 100% of ethyl acetate to 20% acetone/ethyl acetate (v/v)). Concentration in vacuo yielded a pale yellow solid, which was redissolved in acetone (1 mL) and precipitated in an excess of hexane (40 mL). Filtration gave 945 mg (29%) of a pale yellow solid: mp 267−270 °C; ^{1}H NMR (400 MHz, DMSO-d_6) δ 12.82 (s, 2H, H_3), 8.15 (d, 4H, J = 8.0, $H_{2'}$, $H_{6'}$), 7.50−7.90 (m, 6H, H_4, H_6, H_7), 7.13 (d, 4H, J = 8.0, $H_{3'}$, $H_{5'}$), 3.85 (s, 6H, OCH_3); ^{13}C NMR (DMSO-d_6) δ 160.6, 151.9, 144.6, 143.2, 135.7, 135.2, 127.9, 122.7, 118.6, 116.5, 114.3, 55.3; MS (EI^+) *m*/*z* 447 M + H (100), 223 (5); HRMS calcd for $C_{28}H_{23}N_4O_2$ 447.1820, found 447.1827.

4′,4′-[5,5-Bi-1*H*-benzimidazole-2,2-diyl]bisphenol (3). 4,4′-Diamino-3,3′-dinitrobiphenyl (500 mg, 1.82 mmol) in acetone (20 mL) was reduced by hydrogenation using 40 psi of H_2 and a catalytic amount of Raney nickel for 2 h. After filtration the solvent was removed under reduced pressure to obtain a brown solid which was used in the next step without further purification. The crude intermediate and *p*-hydroxybenzaldehyde (445 mg, 3.64 mmol) were heated in nitrobenzene (5 mL) at 150 °C under argon for 12 h. An excess of hexane (50 mL) was added to the cooled mixture to afford a precipitate and this was removed by filtration. The precipitate was then purified by column chromatography on silica gel (gradient from 100% ethyl acetate to 10% methanol/ethyl

acetate (v/v)). Concentration in vacuo afforded a pale yellow solid. This solid was redissolved in acetone (1.5 mL) and an excess of hexane (35 mL) was added to yield a precipitate. Filtration afforded 175 mg (23%) of a pale yellow solid: mp 256−260 °C; ^{1}H NMR (250 MHz, DMSO-d_6) δ 12.71 (s, 2H, H_3), 9.97 (s, 2H, OH), 8.03 (d, 4H, J = 8.6, $H_{3'}$, $H_{5'}$), 7.48−7.88 (m, 6H, H_4, H_6, H_7), 6.93 (d, 4H, J = 8.6, $H_{2'}$, $H_{6'}$); ^{13}C NMR (DMSO-d_6) δ 159.1, 152.7, 144.6, 143.1, 135.7, 135.0, 128.1, 121.1, 118.4, 116.3, 115.5; MS (EI$^+$) m/z 419 M + H (30), 107 (100), 66 (25); HRMS calcd for $C_{26}H_{19}N_4O_2$ 419.1507, found 419.1510.

4-(3′,3′-Dimethylamino-1′-propyloxy) benzaldehyde (4). Diethyl azodicarboxylate (9.55 mL, 61.4 mmol) was added dropwise at 0 °C under argon to a solution of *p*-hydroxybenzaldehyde (5 g, 40.94 mmol), 3-dimethylaminopropan-1-ol (7.27 mL, 61.4 mmol) and triphenylphosphine (16.1 g, 61.4 mmol) in THF (100 mL). The mixture was warmed slowly to room temperature and stirred for 3 h. The solvent was removed under reduced pressure and the crude oil obtained purified by column chromatography on silica gel (gradient from 100% DCM to 20% methanol/DCM (v/v)) to give 7.17 g (85%) of a pale yellow oil: ^{1}H NMR (400 MHz, $CDCl_3$) δ 9.88 (s, 1H, H_1), 7.82 (d, 2H, J = 8.8, H_3, H_7), 7.00 (d, 2H, J = 8.8, H_4, H_6), 4.10 (t, 2H, J = 6.4, $H_{1'}$), 2.46 (t, 2H, J = 7.1, $H_{3'}$), 2.26, (s, 6H, NCH_3), 1.99 (tt, 2H, J = 6.4, J = 7.1, $H_{2'}$); ^{13}C NMR ($CDCl_3$) δ 190.8, 164.3, 132.2, 129.8, 115.1, 66.1, 56.1, 45.5, 27.5; MS (EI$^+$) m/z 208 M + H (46), 86 (48), 58 (100); HRMS calcd for $C_{12}H_{18}NO_2$ 208.1337, found 208.1337.

2,2-Bis[4′-(3′-dimethylamino-1″-propyloxy)phenyl]-5,5-bi-1*H*-benzimidazole (5). 4,4′-Diamino-3,3′-dinitrobiphenyl (1.5 g, 5.47 mmol) in acetone (100 mL) was reduced by hydrogenation using 40 psi of H_2 and a catalytic amount of Raney nickel for 3 h. After filtration the solvent was removed under reduced pressure to obtain a brown solid which was used in the next step without further purification. The crude intermediate and 4-(3′-dimethylamino-1′-propyloxy)benzaldehyde (2.27 g, 10.93 mmol) in nitrobenzene (15 mL) were heated at 150 °C under argon for 12 h. The mixture was cooled to room temperature and methanol (100 mL) was added. The solution was then washed with hexane (3 × 100 mL) to remove the excess of nitrobenzene and the methanol extract concentrated in vacuo to give a brown solid. The solid was then purified by column chromatography on silica gel (hexane and a gradient from 50% ethyl acetate/methanol to 4% Et_3N/methanol (v/v)). Concentration in vacuo afforded a solid, which was then redissolved in acetone (40 mL), and an excess of hexane (400 mL). Filtration from the solution of the resulting precipitate yielded 1.126 g (35%) of a yellow solid; mp 218−220 °C; ^{1}H NMR (400 MHz, DMSO-d_6) δ 12.80 (s, 2H, H_3), 8.12 (d, 4H, J = 8.8, $H_{2'}$, $H_{6'}$), 7.49−7.88 (m, 6H, H_4, H_6, H_7), 7.10 (d, 4H, J = 8.8, $H_{3'}$, $H_{5'}$), 4.07 (t, 4H, J = 6.2, $H_{1''}$), 2.35 (t, 4H, J = 6.9, $H_{3''}$), 2.14 (s, 12H, NCH_3), 1.85−1.88 (m, 4H, $H_{2''}$); ^{13}C NMR (DMSO-d_6) δ 160.9, 152.0, 143.3, 136.1, 135.8, 128.9, 123.4, 122.2, 119.8, 119.6, 115.7, 66.9, 56.5, 46.1, 27.7; MS (EI$^+$) m/z 588 M$^+$ (15), 515 (10), 58 (100); HRMS calcd for $C_{36}H_{40}N_6O_2$ 588.3210, found 588.3203.

Biological Studies. 1. Growth Inhibition Assays. Assessment of growth inhibition was performed in a small panel of human ovarian carcinoma cell lines using the sulforhodamine B (SRB) assay.[32] Included in this panel were two sublines possessing acquired resistance to cisplatin (A2780cisR 12-fold resistant and CH1cisR 6-fold resistant)[32] and a subline possessing acquired resistance to doxorubicin (90-fold), through overexpression of P-glycoprotein.[35] This panel is representative of that used by us in several previous preclinical anticancer drug evaluation studies.

The cell lines grew as monolayers in Dulbecco's modified Eagle's medium containing 10% fetal bovine serum (Imperial Laboratories, Andover, U.K.) supplemented with 2 mM glutamine and 0.5 μg/mL hydrocortisone in 6% CO_2/94% air. The compound was dissolved in 10% dimethyl sulfoxide. Cells were seeded into 96-well microtiter plates at 3000−5000/well and allowed to attach overnight. Serial dilutions of drug in growth medium were then added to quadruplicate wells (with 8 control untreated wells) and left to incubate under normal growth conditions for 96 h, unless otherwise stated. The medium was then removed and wells fixed with 10% trichloroacetic acid and stained with 0.4% SRB in 1% acetic acid as described previously.[32] Basic amino acid content in each well was then measured by solubilizing the bound SRB with 10 mM Tris and using a Titertek Multiscan MCC/340 MKII plate reader set at 540 nm. Mean absorbance was then expressed as a percentage of the control untreated well absorbance and plotted vs drug concentration. Comparisons were made in terms of IC_{50} values (the concentration that reduced the mean absorbance to 50% of those in control wells) and resistance factors (RF, the IC_{50} in a resistant subline versus its parent line).

Where the effect of time of drug exposure was investigated, drug was removed by aspiration at the times indicated (2, 6, 24, and 96 h) and replaced with fresh growth medium and incubated for the remainder of the 96-h period.

2. Hollow Fiber Assay. The hollow fiber assay was used for the initial in vivo evaluation of the compound.[36] The CH1 ovarian cell line was prepared by trypsinization and seeded at 1 × 10^7 single cells/mL into 2-cm polyvinylidene fluoride (PVDF) fibers (Spectrum, Laguna Hills, CA) and heat-sealed. Three days later, following incubation of fibers in growth medium, fibers were implanted into the peritoneal cavity (ip) of nude mice using a trochar. One day later (day 4 after seeding into fibers), mice were treated with either a single maximum tolerated dose of compound **5** (4 mg/kg, ip administration) or vehicle (10% DMSO/90% arachis oil). Six days later, fibers were removed and the numbers of viable cells assessed in treated versus control fibers using the colorimetric MTT assay and measuring absorbance at 540 nm.[36] Results are expressed as a % treated/control absorbance.

3. Human Tumor Xenograft Studies. Tumor fragments from the CH1 human ovarian xenograft (corresponding to the CH1 cell line) were implanted sc into the flanks of adult female nude mice. Animals bearing established tumors (largest diameter of 6−8 mm) were then randomized (day 0) into treatment groups of 6 mice to receive either compound X (at the predetermined maximum tolerated dose of 4 mg/kg) or vehicle (10% DMSO/90% arachis oil). Animals were dosed by ip injection on days 0, 4, and 8 following randomization.

Tumor size was determined twice weekly by caliper measurements, and tumor volumes calculated (volume = $[a \times b^2 \times \pi]/6$, where a and b are orthogonal tumor diameters). Tumor volumes were then expressed as a percentage of the volume at the start of treatment (relative tumor volume). The effect of the drug was assessed in terms of the optimum T/C (the ratio of the mean relative tumor volume of treated to that of control groups) calculated on each day of measurement.

All procedures involving animals were performed within the guidelines set by the Animal Ethics Committee of the Institute of Cancer Research and the United Kingdom Coordinating Committee on the welfare of animals in experimental neoplasia.

Crystallographic Studies. 1. Crystallization and Data Collection. The DNA sequence d(CGCGAATTCGCG), purified by HPLC, was purchased from Oswell Ltd. (Southampton, U.K.). Crystals were grown from hanging drops at 284 K as yellow cubes. The crystal that was used for data collection was grown from a drop containing 1 μL of 4 mM single-stranded DNA dissolved in 40 mM sodium cacodylate buffer, pH 6.8, 1 μL of 2 mM compound **5** (in the same buffer) and 2 μL of Hampton Screening kit reagent number 16, consisting of 10% 2-methylpentane-2,4-diol (MPD), 12 mM spermine tetrahydrochloride, 80 mM NaCl and 20 mM $MgCl_2$. This drop was equilibrated against 700 μL of 35% MPD solution and the crystal grew over a period of 4 weeks. The crystal was flash-frozen in liquid nitrogen and the data were collected using a Rigaku RAXIS-IV image plate detector using mirror-focused Cu Kα radiation from a Rigaku RU200 rotating-anode generator. The crystal−detector distance was 100 cm and the oscillation range was 1.5°, leading to data collection at maximum resolution of 2.0 Å. 40 frames were collected and

Table 2. Crystallographic Data

wavelength (Å)	1.542
unit cell dimensions	$a = 25.15$ Å, $\alpha = 90°$ $b = 39.94$ Å, $\beta = 90°$ $c = 65.65$ Å, $\chi = 90°$
space group	$P2_12_12_1$
no. of reflections	4862
no. of unique reflections	4664
no. of reflections used in refinement	4198
no. of parameters refined	2465
restraints	3856
no. of atoms in DNA	486
no. of full-occupancy waters	70
no. of half-occupancy waters	15
no. of magnesium ions	1
max resolution of obsd reflections (Å)	2.0
max resolution of refinement (Å)	2.0
R factor (%)	24.4
R_{free} (%)	30.0

the crystal did not appear to decay during collection. Data reduction and scaling were carried out using the DENZO and SCALEPACK programs.[37] Data collection statistics are given in Table 2.

2. Structure Solution and Refinement. The structure is isomorphous with other previously determined drug−dodecanucleotide complex structures incorporating the same sequence, and the structure of the native sequence (structure BDL001 in the Nucleic Acid Database) was chosen as a starting point for the analysis. The program XPLOR, version 3.1,[38] was used to carry out positional refinement, initially for individual groups and subsequently for individual atoms. The resolution was progressively increased until the final individual positional refinement included all data to 2.0 Å (2405 reflections), at which point further refinement was carried on with the SHELX-97 program.[39]

A $F_o - F_c$ map was generated and electron density corresponding to the drug could clearly be seen, though the density for the side chain regions was not very well-defined. The three-dimensional structure for compound **5** was built with the INSIGHTII package. Refinement was continued after introduction of the drug as well as a dictionary of the drug geometry. A hydrated magnesium ion was located in close proximity to T17, as observed previously in other minor groove structures. A total of 79 solvent molecules were located, of which 65 had full occupancy, according to standard criteria. The side chains of the drug molecule had high temperature factors throughout the refinement, which contributed to the final R and R_{free} values being somewhat greater than normal: 24.4% and 30.0%, respectively. DNA helicoidal parameters were generated with the program CURVES.[29] Coordinates and structure factors have been deposited with the Nucleic Acid Database[41] as entry no. DD0036.

Acknowledgment. We are grateful for support from the Cancer Research Campaign (L.R.K.: Grant No. SP/DC/STU2330/0201; S.N.: Grant No. SP1384). Y. O.-B and A. B. thank the Government of Ghana and the Royal Society of Chemistry Adrien Albert Bequest, respectively, for studentships. We thank P. Rogers, F. Boxall, M. Valenti, and L. Brunton for technical assistance with SRB, hollow fiber, and xenograft assays. We thank the Developmental Therapeutics Program of the National Cancer Institute, Bethesda, MD, for the hollow fiber data.

References

(1) Boykin, D. W.; Kumar, A.; Spychala, J.; Zhou, M.; Lombardy, R. J.; Wilson, W. D.; Dykstra, C. C.; Jones, S. K.; Hall, J. E.; Tidwell, R. R.; Laughton, C.; Nunn, C. M.; Neidle, S. Dicationic Diaryl Furans as anti-*Pneumocystis carinii* Agents. *J. Med. Chem*. **1995**, *38*, 912−916.

(2) Trent, J. O.; Clark, G. R.; Kumar, A.; Wilson, W. D.; Boykin, D. W.; Hall, J. E.; Tidwell, B. L.; Blagburn, B. L.; Neidle, S. Targeting the Minor Groove of DNA: Crystal Structures of Two Complexes between Furan Derivatives of Berenil and the DNA Dodecamer d(CGCGAATTCGCG)$_2$. *J. Med. Chem*. **1996**, *39*, 4554−4562.

(3) Boykin, D. W.; Kimar, A.; Xiao, G.; Wilson, W. D.; Bender, B. C.; McCurdy, D. R.; Hall, J. E.; Tidwell, R. T. 2,5-Bis[4-(N-alkylamidino)phenyl]furans as Anti-*Pneumocystis carinii* Agents. *J. Med. Chem*. **1998**, *41*, 124−129.

(4) Francesconi, I.; Wilson, W. D.; Tanious, F. A.; Hall, J. E.; Bender, B. C.; Tidwell, R. R.; McCurdy, D.; Boykin, D. W. 2,4-Diphenyl Furan Diamidines as Novel Anti-*Pneumocystis carinii* Pneumonia Agents. *J. Med. Chem*. **1999**, *42*, 2260−2265.

(5) Neidle, S.; Kelland, L. R.; Trent, J. O.; Simpson, I. J.; Boykin, D. W.; Kumar, A.; Wilson, W. D. Cytotoxicity of Bis(phenylamidinium) Furan Alkyl Derivatives in Human Tumour Cell Lines: Relation to DNA Minor Groove Binding. *Bioorg. Med. Chem. Lett*. **1997**, *7*, 1403−1408.

(6) Marchini, S.; Ciro, M.; Gallinari, F.; Geroni, C.; Cozzi, P.; Dincalci, M.; Broggini, M. Alpha-bromoacryloyl Derivative of Distamycin A (PNU 151807): a New Noncovalent Minor Groove DNA Binder with Antineoplastic Activity. *Br. J. Cancer* **1999**, *80*, 991−997.

(7) Reddy, B. S. P.; Sondhi, S. M.; Lown, J. W. Synthetic DNA Minor Groove-Binding Drugs. *Pharmacol. Ther*. **1999**, *84*, 1−111.

(8) Lammler, G.; Herzog, H.; Saupe, E.; Schutze, H. R.; Chemotherapeutic Studies on Litomosodoides carini Infection of Mastomys nataleusis 1. The Filaricidal Action of 2,6-bis-Benzimidazoles. *WHO Bull*. **1971**, *44*, 751−756.

(9) Kraut, E. H.; Masspeis, L.; Bakerzak, S.; Grever, M.; Evaluation of Pibenzimol (NSC322921) in Refractory Solid Malignancies. *Proc. Am. Soc. Clin. Oncol*. **1988**, *7*, 62.

(10) Kraut, E.; Fleming, T.; Segal, M.; Neidhart, J.; Behrens, B. C.; MacDonald, J. Phase II Study of Pibenzimol in Pancreatic Cancer − a Southwest Oncology Group Study. *Invest. New Drugs* **1999**, *9*, 95−96.

(11) Ferguson, L. R.; Denny, W. A. Microbial Mutagenic Effects of the DNA Minor Groove Binder Pibenzimol (Hoechst 33258) and a Series of Mustard Analogues. *Mutat. Res*. **1995**, *329*, 19−27.

(12) Turner, P. R.; Denny, W. A. The Mutagenic Properties of DNA Minor-groove Binding Ligands. *Mutat. Res*. **1996**, *355*, 141−169.

(13) Chiang, S.-Y.; Welch, J.; Rauscher, F. J. III.; Beerman, T. A. Effects of Minor Groove Binding Drugs on the Interaction of TATA Box Binding Protein and TFIIA With DNA. *Biochemistry* **1994**, *33*, 7033−7040.

(14) Chen, A. Y.; Chiang, Y.; Gatto, B.; Liu, L. F. DNA Minor Groove-binding Ligands: a Different Class of Mammalian DNA Topoisomerase I Inhibitors. *Proc. Natl. Acad. Sci. U.S.A*. **1993**, *90*, 8131−8135.

(15) Harshman, K. D.; Dervan, P. B. Molecular Recognition of B-DNA by Hoechst 33258. *Nucleic Acids Res*. **1985**, *13*, 4825−4835.

(16) Spink, N.; Brown, D. G.; Skelly, J. V.; Neidle, S. Sequence Dependent Effects in drug−DNA Interaction: the Crystal Structure of Hoechst 33258 Bound to the d(CGCAAATTTGCG)$_2$ Duplex. *Nucleic Acids Res*. **1994**, *22*, 1607−1612.

(17) Vega, M. C.; Coll, M.; Aleman, C. Intrinsic Conformational Preferences of the Hoechst Dye Family and their Influence on DNA Binding. *Eur. J. Biochem*. **1996**, *239*, 376−383.

(18) Parkinson, J. A.; Barber, J.; Douglas, K. T.; Rosamond, J.; Sharples, D. Minor-groove Recognition of the Self-complementary Duplex d(CGCGAATTCGCG)$_2$ by Hoechst 33258: a High-field NMR Study. *Biochemistry* **1990**, *29*, 10181−10190.

(19) Embrey, K. J.; Searle, M. S.; Craik, D. J. Interaction of Hoechst 33258 with the Minor Groove of the A + T-rich DNA duplex d(GGTAATTACC)$_2$ Studied in Solution by NMR Spectroscopy. *Eur. J. Biochem*. **1993**, *211*, 437−447.

(20) Czarny, A.; Boykin, D. W.; Wood, A. A.; Nunn, C. M.; Neidle, S.; Zhao, N.; Wilson, W. D. Analysis of van der Waals and Electrostatic Contributions in the Interactions of Minor-Groove Binding Benzimidazoles with DNA. *J. Am. Chem. Soc*. **1995**, *117*, 4716−4717.

(21) Wood, A. A.; Nunn, C. M.; Czarny, A.; Boykin, D. W.; Neidle,S. Variability in DNA Minor Groove Width Recognised by Ligand Binding. The Crystal Structure of a bis-Benzimidazole Compound Bound to the DNA Duplex d(CGCGAATTCGCG)$_2$. *Nucleic Acids Res*. **1995**, *23*, 3678−3684.

(22) Clark, G. R.; Squire, C. J.; Gray, E. J.; Leupin, W.; Neidle, S. Designer DNA-Binding Drugs: The Crystal Structure of a *meta*-Hydroxy Analogue of Hoechst 33258 bound to d(CGCGAATTCGCG)$_2$. *Nucleic Acids Res*. **1996**, *24*, 4882−4889.

(23) Clark, G. R.; Boykin, D. W.; Czarny, A.; Neidle, S. Structure of a bis-amidinium derivative of Hoechst 33258 complexed to the dodecanucleotide d(CGCGAATTCGCG)$_2$: the role of hydrogen bonding in minor groove drug−DNA recognition. *Nucleic Acids Res*. **1997**, *25*, 1510−1515.

(24) Clark, G. R.; Gray, E. J.; Li, Y.-H.; Leupin, W.; Neidle, S. Isohelicity and Phasing in Drug−DNA sequence recognition: Crystal Structure of a Tris (Benzimidazole)−Oligonucleotide Complex. *Biochemistry* **1996**, *35*, 13745−13752.
(25) Pilch, D. S.; Xu, Z.; Sun, Q.; LaVoie, E. J.; Liu, L. F.; Breslauer, K. J. A Terbenzimidazole that Preferentially Binds and Conformationally Alters Structurally Distinct DNA Duplex Domains: a Potential Mechanism for Topoisomerase I Poisoning. *Proc. Natl. Acad. Sci. U.S.A.* **1997**, *94*, 13565−13570.
(26) Kim, J. S.; Sun, Q.; Chaing, Y.; Liu, A.; Liu, L. F.; LaVoie, E. J. Quantitative Structure−activity Relationships on 5-substituted Terbenzimidazoles as Topoisomerase I Poisons and Antitumor Agents. *Bioorg. Med. Chem.* **1998**, *6*, 163−172.
(27) Xu, Z.; Tsai-Kun, L.; Kim, J. S.; LaVoie, E. J.; Breslauer, K. L.; Liu, L. F.; Pilch, D. S. DNA Minor Groove Binding-directed Poisoning of Human DNA Topoisomerase I by Terbenzimidazoles. *Biochemistry* **1998**, *37*, 3558−3566.
(28) Neidle, S.; Mann, J.; Rayner, E. L.; Baron, A.; Opoku-Boachen, Y.; Simpson, I. J.; Smith, N. J.; Fox, K. R.; Hartley, J. A.; Kelland, L. R. Symmetric bis-Benzimidazoles, a New Class of Sequence-Selective DNA-binding Molecules. *J. Chem. Soc., Chem. Commun.* **1999**, 929−930.
(29) Lavery, R.; Sklenar, H. Defining the Structure of Irregular Nucleic Acids − Conventions and Principles. *J. Biomol. Struct. Dyn.* **1989**, *6*, 655−667.
(30) Monks, A.; Scudiero, D. A.; Johnson, G. S.; Paull, K. D.; Sausville, E. A. The NCI Anti-cancer Drug Screen: a Smart Screen to Identify Effectors of Novel Targets. *Anti-Cancer Drug Des.* **1997**, *12*, 533−541.
(31) Hollingshead, M. G.; Alley, M. C.; Camalier, R. F.; Abbott, B. J.; Mayo, J. G.; Malspeis, L.; Grever, M. R. In vivo Cultivation of Tumor cells in Hollow Fibres. *Life Sci.* **1995**, *57*, 131−141.
(32) Kelland, L. R.; Barnard, C. F. J.; Mellish, K. J.; Jones, M.; Goddard, P. M.; Valenti, M.; Bryant, A.; Murrer, B. A.; Harrap, K. R. A Novel *trans*-Platinum Coordination Complex Possessing in vitro and in vivo Antitumor Activity. *Cancer Res.* **1994**, *54*, 5618−5622.
(33) Broggini, M.; D'Incalci, M. Modulation of Transcription factor-DNA Interactions by Anticancer Drugs. *Anti-Cancer Drug Des.* **1994**, *9*, 373−387.
(34) Soderlind, K.-J.; Gorodetsky, B.; Singh, A. K.; Bachur, N. R.; Miller, G. G.; Lown, J. W. Bis-benzimidazole anticancer agents: targeting human tumour helicases. *Anti-Cancer Drug Des.* **1999**, *14*, 19−36.
(35) Sharp, S. Y.; Rowlands, M.; Jarman, M.; Kelland, L. R. Effects of a New Antioestrogen Idoxifene on Cisplatin- and Doxorubicin-sensitive and Resistant Human Ovarian Carcinoma Cell Lines. *Br. J Cancer* **1994**, *70*, 409−414.
(36) Mosmann T, J. Rapid Colorimetric Assay for Cellular Growth and Survival: Application to Proliferation and Cytotoxicity Assays. *Immunol. Methods* **1983**, *65*, 55−63.
(37) Otwinowski, Z.; Minor, W. In *Data Collection and Processing;* Sawyer, L., Isaacs, N. W., Bailey, S., Eds.; SERC Daresbury Laboratory: Warrington, U.K., 1993.
(38) Brünger, A. T.; Kuriyan, J.; Karplus, M. Crystallographic R factor Refinement by Molecular Dynamics. *Science* **1987**, *235*, 458−460.
(39) Sheldrick, G. M. *SHELX-97*, a crystallographic refinement program; University of Göttingen: Germany, Göttingen, 1997.
(40) Nicholls, A.; Sharp, K. A.; Honig, B. Protein Folding and Association: Insights from the Interfacial and Thermodynamic Properties of Hydrocarbons. *Proteins* **1991**, *11*, 281−296.
(41) Berman, H. M.; Olson, W. K.; Beveridge, D. L.; Westbrook, J.; Gelbin, A.; Demeny, T.; Hsieh, S.-H.; Srinivasan, A. R.; Schneider, B. The Nucleic Acid Database: a Comprehensive Relational Database of Three-Dimensional Structures of Nucleic Acids. *Biophys. J.* **1992**, *63*, 751−759.

JM000297B